Cluster-based Priors for MAP PET Image Reconstruction

Lijun Lu, Jing Tang, *Member, IEEE,* Nicolas Karakatsanis, *Member, IEEE,* Wufan Chen, *Senior Member, IEEE,* and Arman Rahmim, *Member, IEEE*

Abstract—We propose two forms of cluster-based priors for the maximum *a Posterior* (MAP) algorithm to improve PET image reconstruction quantitatively. Conventionally, most priors in MAP reconstruction use weighted differences between voxel intensities within a small localized spatial neighborhood, exploiting intensity similarities amongst adjacent voxels. It was hypothesized that by incorporating a larger collection of voxels with similar properties, the MAP approach has a greater ability to impose smoothness while preserving edges. We propose to use clustering techniques as applied to pre-reconstructed images to define clustered neighborhoods of voxels with similar intensities. Two forms of cluster-based priors were proposed. The unweighted cluster-based prior (CP-U) applies a uniform weight regardless of position within a cluster to voxel value differences. The distance weighted cluster-based prior (CP-W) applies different weights based on the distance between voxels within a cluster. The two forms of cluster-based priors, CP-U and CP-W, are implemented within MAP reconstruction. The fuzzy C-means (FCM) method is used to cluster the filtered backprojection (FBP) reconstructed image before MAP reconstruction. To evaluate the proposed priors, a mathematical brain phantom was used in analytic simulations to generate the projection data. We compare reconstructed images from the proposed cluster-based priors MAP algorithms with those from conventional MLEM and quadratic prior (QP) MAP algorithms, using the regional bias (normalized mean squared error, NMSE) vs noise (normalized standard deviation tradeoff, NSD) tradeoff curves. MAP reconstruction using cluster-based priors (CP-U-MAP and CP-W-MAP) dramatically improved the noise vs. bias tradeoff when the number of clusters selected is equal to or larger than the true number of clusters within the image. However, the CP-U-MAP may introduce some bias in a region that may be wrongly clustered, e.g. when the number of selected clusters is smaller than the true number of clusters, a problem that is largely avoided by CP-W-MAP reconstruction which exhibits very robust quantitative performance.

I. INTRODUCTION

Positron emission tomography (PET) is a non-invasive clinical imaging technique for quantitative study of the functional activity of subjects. However, due to low spatial resolution and inherently noisy data, PET reconstruction is an ill-posed problem [1]. Maximum *a Posterior* (MAP) image reconstruction can provide improved spatial resolution and noise properties by using *a priori* information as regularization. Conventional priors focus on local neighborhoods and subsequently penalize inter-voxel intensity differences using a variety of functions including the quadratic prior, median prior [2], and priors whose gradients levels off with increasing differences to allow enhanced tolerance for edges, e.g. the Geman [3], Huber [4], Green [5], and Nuyts [6] priors (the Nuyts prior has the additional advantages of being concave and penalizing relative (not absolute) differences). Nevertheless, a drawback of these conventional priors is that they only consider the local information to define the prior at any given position.

An alternative approach to application of smoothness constraints, while preserving edges, is to penalize inter-voxels differences in uptake based on spatially non-localized neighborhoods with similar intensity. Chen *et al* proposed nonlocal prior for tomographic reconstruction, which penalized inter-voxels differences over broader neighborhood for each voxel, with weights depending on some measure of neighbor similarity between voxels [7]. Although this nonlocal prior showed better performance compared to conventional prior, it required the computationally intense approach of re-evaluating weights at every iteration. In the different context of post-reconstruction PET/SPECT image analysis, a number of clustering-based techniques were previously proposed to better facilitate segmentation [8]–[12]. We think the clustering based techniques can be used for prior definition In this work, the fuzzy C-means (FCM) algorithm was used to group voxels into clusters, as initially obtained using initial reconstruction. Then MAP reconstruction was performed wherein we proposed and evaluated two forms of priors: The unweighted cluster-based prior (CP-U) and the distance weighted cluster-based prior(CP-W), as elaborated in the next section.

II. METHODS

A. MAP Reconstruction

Let **f** and **g** be vectors representing the image voxels and projection measurements, respectively. The MAP estimate of image **f** from measurements **g** is given by

$$\widehat{\mathbf{f}} = \underset{\mathbf{f} \geq 0}{\arg\max} \frac{P(\mathbf{g}|\mathbf{f})P(\mathbf{f})}{P(\mathbf{g})}, \tag{1}$$

where $P(\mathbf{g}|\mathbf{f})$ is the likelihood function, $P(\mathbf{f})$ and $P(\mathbf{g})$ are the *a priori* probability distributions of the image and the projection measurements respectively. We assume that the prior $P(\mathbf{f})$ follows a Gibbs form:

$$P(\mathbf{f}) \propto \exp\{-\beta U(\mathbf{f})\}, \qquad (2)$$

where $U(\mathbf{f})$ is the energy function, which has conventionally been utilized to penalize inter-voxel intensity variations within a small local neighborhood. β is a positive constant that control the noise properties of the reconstructed image.

Seeking the solution of $\mathbf{f}$ to (1) is equivalent to finding $\widehat{\mathbf{f}}$ that maximizes the log-posterior probability:

$$\log P(\mathbf{g}|\mathbf{f}) - \beta U(\mathbf{f}). \qquad (3)$$

Modeling poisson statistics, we invoke the one-step-late (OSL) approximation for an iterative update to the MAP estimate [5] :

$$f_j^{new} = \frac{f_j^{old}}{\sum_i a_{ij} + \beta \frac{\partial U(f)}{\partial f_j}\big|_{f_j = f_j^{old}}} \sum_i \frac{a_{ij} g_i}{\sum_j a_{ij} f_j^{old}}, \qquad (4)$$

where g_i denotes the projection-data element i of the measured emission data $\mathbf{g}$, a_{ij} represent the element of the projection matrix $\mathbf{A}$, denoting the probability of a positron emitted from voxel j resulting in a coincidence at the ith line of response. At each iteration, the new estimate of voxel j in the image $\mathbf{f}$ is updated from the old estimate.

B. Cluster-based Priors

Conventionally, the prior is computed via a weighted summation of differences between voxel intensities within a small local neighborhood. In order to make use of more voxels to further encourage smoothing, while preserving edges and gradients, we expanded the use of localized neighborhoods to those containing all voxels with similar intensities as clustered together. Here we propose two forms of cluster-based priors.

Unweighted cluster-based prior:

$$U_1(f) = \sum_j \sum_{k \in c\{j\}} \frac{1}{N_{c\{j\}} - 1} (f_j - f_k)^2, \qquad (5)$$

where $c\{j\}$ represents the cluster in which voxel j is grouped, and $N_{c\{j\}}$ is the number of voxels in cluster $c\{j\}$.

However, due to noise and/or using insufficient number of clusters, some voxels may be incorrectly clustered together, and lead to bias in the MAP reconstructed images. Subsequently, a methodology was developed to alleviate such a bias: namely, distance weighting was introduced to reduce the resulting adverse impact, as elaborated next.

Distance weighted cluster-based prior:

$$U_2(f) = \sum_j \sum_{k \in c\{j\}} w_{jk} (f_j - f_k)^2, \qquad (6)$$

where w_{jk} is inversely proportional to the distance between voxel j and voxel k. In such a scenario, we only need to compute w_{jk} in a large neighborhood (e.g. 9×9), and not the entire cluster, as the weights of voxel out of this large neighborhood will be very small. In turn, this can lead to considerable computational speed-up.
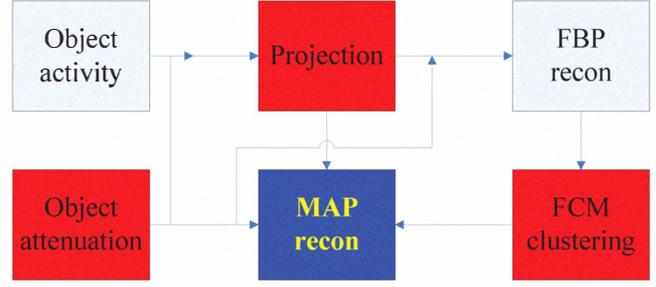

Fig. 1. Flowchart of proposed reconstruction algorithm.

C. The Flowchart of the Proposed Reconstruction Algorithm

There are two steps in the reconstruction. First, the FCM method is used to cluster the FBP reconstructed image. Second, MAP reconstruction using the cluster-based prior is performed. This is depicted in Fig.1.

D. Human Brain PET Simulation

We used a mathematical human brain phantom [13] for the purpose of performing realistic simulations. For the two-dimension image reconstruction, we simulated a PET scanner operating in two-dimensional model producing projection data with 130 radial bins and 192 angle views over $180°$. Image reconstruction was performed with MAP using the two forms of cluster-based prior using different number of clusters, as well as conventional MLEM and MAP using the conventional quadratic prior (QP-MAP).

E. Evaluation Metrics

To quantitatively evaluate the reconstructed images, we used the normalized mean square error (NMSE), as a measure of bias, and the normalized standard deviation (NSD), as a measure of noise, for individual areas of the brain. The NMSE for each ROI covering one area of the brain was calculated using

$$\mathrm{NMSE} = \frac{1}{R} \sum_{j=1}^{R} \left(\frac{\bar{f}^r - \bar{\mu}}{\bar{\mu}} \right)^2, \qquad (7)$$

where $\bar{f}^r = \frac{1}{n} \sum_{i=1}^{n} f_i^r$ and $\bar{\mu} = \frac{1}{n} \sum_{i=1}^{n} \mu_i$; f_i^r denotes the ith reconstructd voxel intensity from rth noise realization and μ denotes the reference true activity value; n is the number of voxel in the ROI and R is the number of noise realizations. We adopted such an ROI-based definition as we believe it should minimize the effect of voxel noise on the bias-measuring metric. For each ROI, the NMSE bias value was plotted against the NSD noise value, as calculated using

$$\mathrm{NSD} = \frac{1}{n} \sum_{i=1}^{n} \frac{\sqrt{\frac{1}{R-1} \sum_{r=1}^{R} (f_i^r - \bar{f}_i)^2}}{\bar{f}_i}, \qquad (8)$$

where f_i^r , n and m are defined as those in (7); $\bar{f}_i = \frac{1}{R} \sum_{r=1}^{R} f_i^r$ represents the ensemble mean value of voxel i.
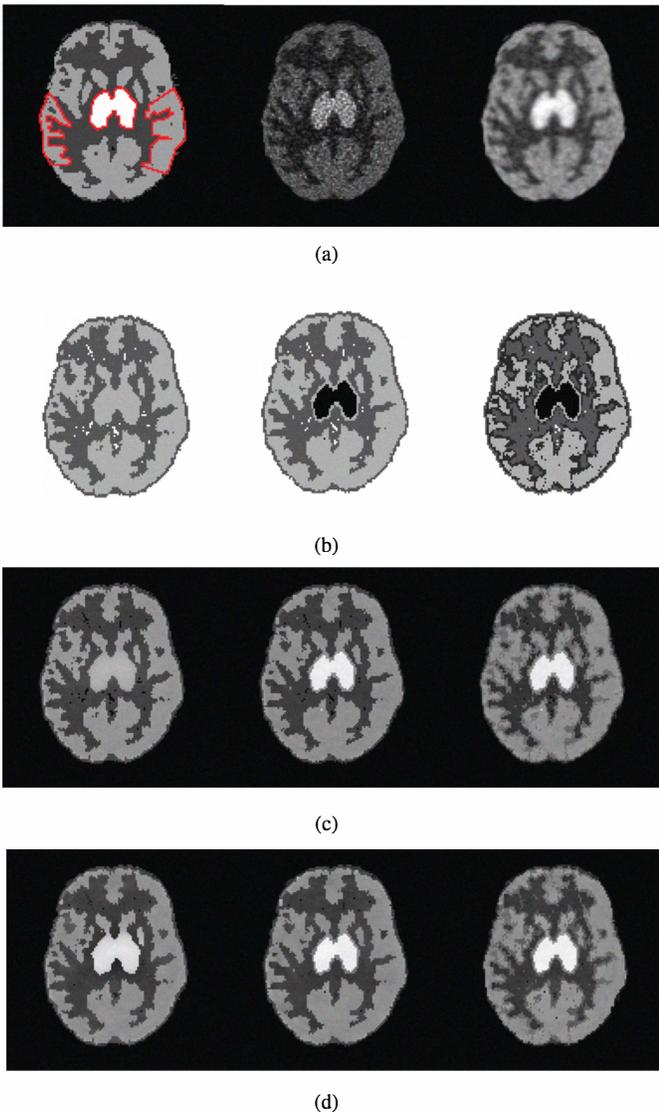
(a)

(b)

(c)

(d)

Fig. 2. The true image, the clustered images and the reconstructed images. (a) The true image and conventional reconstructions (from left to right: the phantom, reconstructed images using ML-EM, QP-MAP), (b) Clustered images from initial FBP reconstruction (from left to right: using 3 clusters, 4 clusters, 5 clusters); the true number of clusters (i.e. number of different uptake regions in the original phantom) were 4, (c) CP-U-MAP reconstructed images using clustered images in (b), respectively, (d) CP-W-MAP reconstructed images using clustered images in (b), respectively.

III. RESULTS

A. Reconstructed Images

In Fig. 2, we show the phantom image, the clustered images and the reconstructed images. In Fig. 2. (a), the center region and the two side regions labeled by red line indicate the thalamus and temporal gyrus, respectively. We can see that reconstructions using cluster-based priors (CP-U-MAP and CP-W-MAP) with the correct number of clusters (i.e. 4) exhibit excellent performance in suppressing noise and preserving edges. If the cluster number is less than the true number of clusters, the reconstructed image using CP-U-MAP may introduce some bias as demonstrated in Fig. 2. (c), while CP-W-MAP has better performance visually.

B. Bias-Noise Curve

In Fig. 3, we provide quantitative evaluation of the two proposed cluster-based priors (CP-U-MAP and CP-W-MAP) when utilizing different number of clusters. Of particular interest is when insufficient number of clusters (i.e. 3) are used, merging the thalamus into regions of different uptake(shown in Fig. 2. (b)). For different number of clusters, Fig. 3 depicts bias (NMSE) vs. noise (NSD) trade-off curves for the thalamus and temporal gyrus, as generated using an increasing number of iterations. We can see that if the cluster number is equal to or more than the true number of clusters, both CP-U-MAP and CP-W-MAP have better performance than conventional QP-MAP and MLEM (shown in Fig. 3. (b)-(c) and (e)-(f)). However, when the cluster number is less than the true number of clusters, the CP-U-MAP may introduce larger bias than conventional QP-MAP and MLEM, while CP-W-MAP demonstrates the best quantitative performance (shown in Fig. 3. (a)).

IV. DISCUSSION

Fuzzy C-means (FCM) algorithm was used as applied to pre-reconstructed images to defined clustered neighborhoods of voxels with similar intensities. In this study, we limited the range of cluster numbers from 3 to 5 and applied the clustering algorithm to group voxels together. Two forms of cluster-based priors were proposed and evaluated. It was illustrated that reconstructions using the new priors (CP-U-MAP and CP-W-MAP) with correct or slightly over estimated number of clusters (i.e. 4-5) exhibit excellent performance in suppressing noise and preserving edges. If the number of clusters were less than the true number of clusters, the reconstructed image using CP-U-MAP could introduce some bias.

The true number of clusters is usually not known *a priori*. Therefore one faces the difficult issue of choosing the number of clusters. In the work by Belhassen and Zaidi [11], the number of clusters is computed by optimizing the Bayesian information criterion (BIC). Wong *et al* [14] used two information theoretic criteria, namely, Akaike information criterion (AIC) and Schwarz criterion (SC, which is equivalent to BIC) to determine the number of clusters to use. AIC and BIC invoke different statistical models [15], and in our future work we will compare their performance as applied to our proposed methods.

V. CONCLUSION

A MAP image reconstruction method using cluster-based priors that improves the quantification of PET image was developed and evaluated. The simulation study illustrates that cluster-based MAP reconstruction results in quantitatively enhanced images compared to conventional MAP reconstruction using localized prior. The CP-W may be a more robust prior than the CP-U, if some voxels are incorrectly clustered.
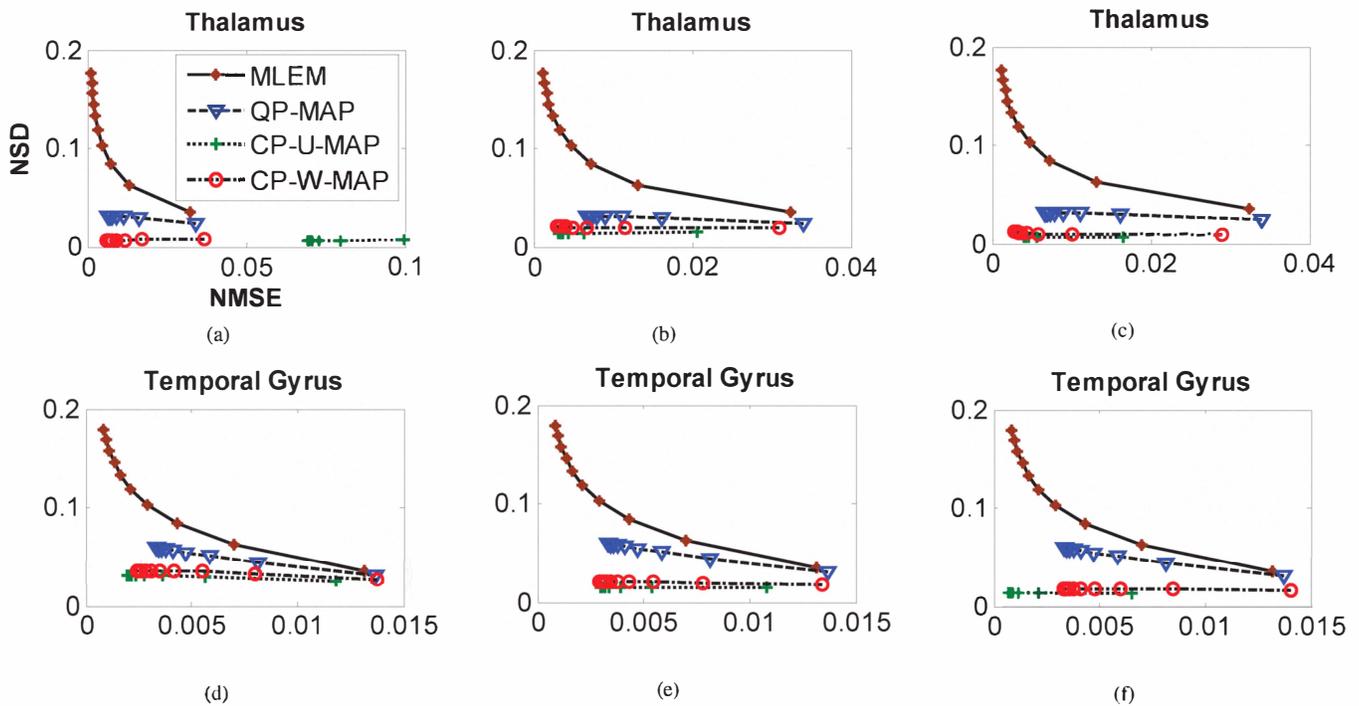
Fig. 3. NMSE (bias) versus NSD (noise) trade-off for different ROIs, with increasing iteration (from left to right: 3 clusters, 4 clusters and 5 clusters): (a)-(c) Thalamus region, (e)-(f) Temporal Gryus region.

REFERENCES

[1] A. Rahmim and H. Zaidi, PET versus SPECT: strengths, limitations and challenges, *Nucl. Med. Commun.*, vol. 29, pp. 193-207, 2008.

[2] I. T. Hsiao, A. Rangarajan and G. R. Gindi, A new convex edgepreserving median prior with applications to tomography. *IEEE Trans. Med. Imaging*, vol. 22, pp. 580C585, 2003.

[3] S. Geman and D. E. McClure, Statistical methods for tomographic image reconstruction. *Proceedings of the 46th Session of the International Statistical Institute*, vol. 52, pp. 5-21, 1987.

[4] E. U. Mumcuoglu, R. M. Leahy and S. R. Cherry, Bayesian reconstruction of PET images: methodology and performance analysis, *Phys. Med. Biol.*, vol. 41, pp. 1777-1807, 1996.

[5] P. J. Green, Bayesian reconstructions from emission tomography data using a modified EM algorithm, *IEEE Trans. Med. Imaging*, vol. 9, pp. 84-93, 1990.

[6] J. Nuyts, D. Beque, P. Dupont and L. Mortelmans, A concave prior penalizing relative differences for maximum-a-posteriori reconstruction in emission tomography, *IEEE Trans. Nucl. Sci.*, vol. 49, pp. 56-60, 2002.

[7] Y. Chen, J. Ma, Q. Feng, L. Luo, P. Shi and W. Chen, Nonlocal prior Bayesian tomographic reconstruction, *J. Math. Imaging Vis.*, vol. 30, pp. 133-146, 2008.

[8] P. D. Acton, L. S. Pilowsky, H. F. Kung and P. J. Ell, Automatic segmentation of dynamic neuroreceptor single-photon emission tomography images using fuzzy clustering, *Eur. J. Nucl. Med. Mol. Imaging*, vol. 26, pp. 581-590, 1999.

[9] H. Zaidi, M. Diaz-Gomez, A. O. Boudraa, and D. O. Slosman, Fuzzy clustering-based segmented attenuation correction in whole-body PET imaging, *Phys. Med. Biol.*, vol. 47, pp. 1143C1160, 2002.

[10] W. Zhu and T. Jiang, Automation segmentation of PET image for brain tumors, *IEEE Nucl. Sci. Symp. Conf. Record*, vol. 4, pp. 2627-2629, 2003.

[11] S. Belhassen and H. Zaidi, A novel fuzzy C-means algorithm for unsupervised heterogeneous tumor quantification in PET, *Med. Phys.*, vol. 37, pp. 1309-1324, 2010.

[12] A. E. O. Boudraa, J. Champier, L. Cinotti, J. C. Bordet, F. Lavenne and J. J. Mallet, Delineation and quantitation of brain lesions by fuzzy clustering in positron emission tomography, *Comput. Med. Imag. Grap.*, vol. 20, pp. 31-41, 1996.

[13] A. Rahmim, K. Dinelle, J. C. Cheng, M. A. Shilov, W. P. Segars and S. C. Lidstone, Accurate event-driven motion compensation in high-resolution PET incorporating scattered and random events, *IEEE Trans. Med. Imaging*, vol. 27, pp. 1018-1033, 2008.

[14] K. P. Wong, D. Feng, S. R. Meikle and M. J. Fulham, Segmentation of dynamic PET images using cluster analysis, *IEEE Trans. Nucl. Sci.*, vol. 49, pp. 200-207, 2002.

[15] G. Schwarz, Estimating the dimension of a model, *Ann. Stat.*, vol. 6, pp. 461-464, 1978.